PRAMANA
— journal of
physics

© Printed in India

Vol. 46, No. 6,
June 1996
pp. 431–449

Positron scattering from hydrocarbons

RITU RAIZADA and K L BALUJA
Department of Physics and Astrophysics, University of Delhi, Delhi 110 007, India

MS received 29 January 1996

Abstract. The total cross sections for positron impact on hydrocarbons have been calculated using the additivity rule in which the total cross section for a molecule is the sum of the total cross section for the constituent atoms. The energy range considered is from a few eV to several thousand eV. The total cross sections for positron impact on an atom are calculated by employing a complex spherical potential which comprises of a static, polarization and an absorption potential. We have good agreement with the experimental results for hydrocarbons for positron energy $\geqslant 100$ eV. Our results also agree with the available calculations for CH_4 and C_2H_2 which employed full molecular wavefunctions beyond 100 eV. Our absorption cross sections also agree with molecular wave-function calculations for C_2H_2 and CH_4 beyond 100 eV. We have shown the Bethe plots for e^+–C and e^+–H scattering systems and Bethe parameters have been extracted. We have fitted the cross section for positron impact on hydrocarbons in the form $\sigma_t(C_nH_m) = naE^{-b} + mcE^{-d}$ in the energy range 300–5000 eV where $a = 195{\cdot}0543$, $b = 0{\cdot}7986$, $c = 371{\cdot}1757$ and $d = 1{\cdot}1379$ with E in eV and σ_t in 10^{-16} cm^2.

Keywords. Positron; hydrocarbons; static potential; polarization potential; absorption potential; inelastic and total cross sections; Bethe plot; independent atom model; additivity rule.

PACS Nos 34·80; 34·90

1. Introduction

The total cross sections (including elastic plus energetically possible all inelastic channels) for positron scattering from various molecules have recently been measured for energy ranging from a few eV to several hundred eV in various laboratories. The experimental and theoretical data have been summarized earlier [1–5]. The surge in experimental activity is due to the availability of positron beams of good intensity and the ease with which the positrons can be detected.

The comparison between positron and electron scattering data on a particular target gives better insight into the scattering mechanism. The effect of polarization is more important in the case of positron scattering because of the cancellation effects between the repulsive static potential and the attractive polarization potential. Due to the lack of symmetry of the molecule, there are additional degrees of freedom like rotation and vibration. At low impact energies, the effect of positronium formation must be taken into account. At intermediate energies, some inelastic channels are open and it is a formidable task to include all of these channels explicitly in the scattering calculation. Due to these physical constraints, an optical potential model approach [1] is found to be adequate in predicting the total cross sections. In brief, the many channel problem is

reduced to a single channel problem. In spite of this simplicity, the task is still difficult due to the lack of availability of wavefunctions of complex molecules like hydrocarbons. However, at high energies, an independent atom model [6] has often been used to calculate the elastic cross sections. In this model, the constituent atoms are considered as separate scattering systems and interference occurs between the electron waves scattered by individual atoms. The interference term is dependent upon the geometry of the molecule. The inelastic effects within the independent atom model can be incorporated by using the optical theorem [7]. This leads to great simplification in which the total cross section for positron impact on a molecule can be expressed as an incoherent sum over the total cross sections of the consitituent atoms. This additivity rule has been used earlier for electron impact on various atoms and molecules [8–11]. The validity of additivity rule has also been studied for electron-impact ionization cross sections [12].

The present work deals with the calculation of total cross sections for positron impact on hydrocarbons by employing the additivity rule. The total cross-sections for carbon and hydrogen atoms can be conveniently calculated by an optical potential method [13]. This method takes into account positron-atom interaction to all orders of the perturbation. The total cross sections for positron impact on various hydrocarbons have been experimentally measured [14–17].

2. Theory

The positron-atom scattering system is described by the Schrödinger equation

$$(H+V)\psi(\mathbf{r}_1,\ldots,\mathbf{r}_N,\mathbf{r}) = E\psi(\mathbf{r}_1,\ldots,\mathbf{r}_N,\mathbf{r}), \tag{1}$$

where the total wavefunction of the N target electrons ($\mathbf{r}_N$) and the positron ($\mathbf{r}$) is expanded in terms of channel functions Φ_i,

$$\psi(\mathbf{r}_1,\ldots,\mathbf{r}_N,\mathbf{r}) = \sum_{i=1}^{M} \Phi_i(\mathbf{r}_1,\ldots,\mathbf{r}_N)F_i(\mathbf{r}), \tag{2}$$

where M is the number of channels included. After expanding $F_i(\mathbf{r})$ in terms of Legendre polynomials, the radial part for each partial wave satisfies the coupled equation

$$\left(\frac{\mathrm{d}^2}{\mathrm{d}r^2} - \frac{l_i(l_i+1)}{r^2} + k_i^2\right)F_i(r) = 2\sum_j U_{ij}(r)F_j(r), \tag{3}$$

where $U_{ij}(r)$ is the coupling potential given by

$$U_{ij}(r) = \frac{Z}{r}\delta_{ij} - \sum_{k=1}^{M}\left\langle \Phi_i\left|\frac{1}{|\mathbf{r}_k-\mathbf{r}|}\right|\Phi_j\right\rangle. \tag{4}$$

Z is the nuclear charge of the atom, H is the atomic hamiltonian and k_i is the wave number in the ith channel.

At intermediate and high positron impact energies, we replace $\Sigma_j U_{ij}(r)F_j(r)$ by $V_{\text{opt}}(r)F(r)$ where $V_{\text{opt}}(r)$ is a local optical model potential. In this case, our many

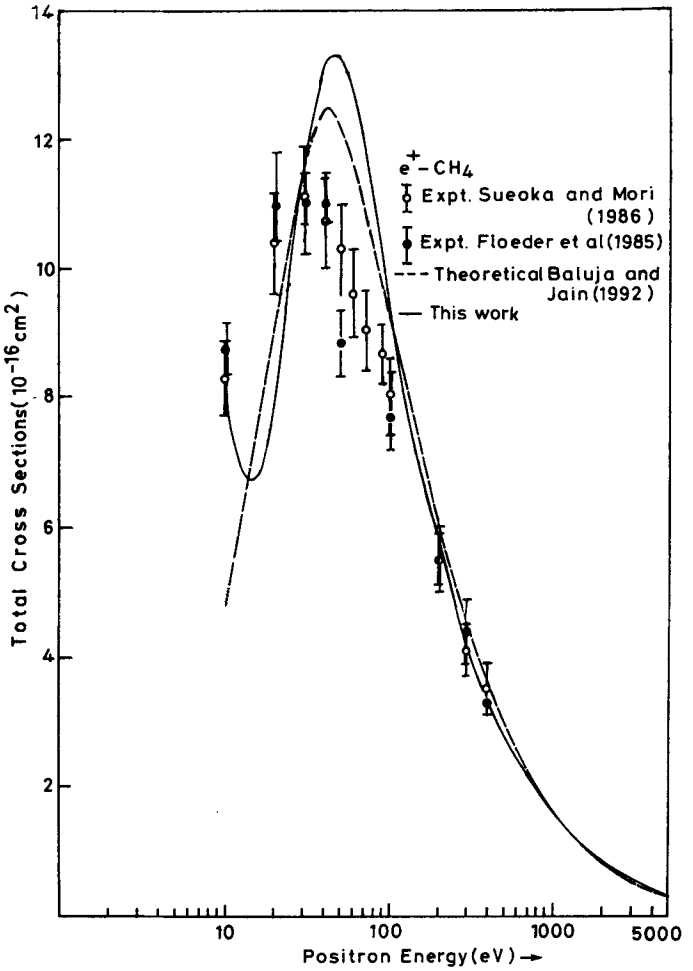

Figure 1. Total cross-sections for positron impact on CH_4.

channel problem is reduced to a single channel problem and we can replace eq. (3) by

$$\left[\frac{d^2}{dr^2} - \frac{l(l+1)}{r^2} + k^2 - 2V_{opt}(r)\right] F(r) = 0 \tag{5}$$

when all the channels are closed, $V_{opt}(r)$ is real which becomes complex when some channels are open. The imaginary part of $V_{opt}(r)$ then accounts for absorption effects due to loss of flux in the open channels. We express $V_{opt}(r)$ as [18]

$$V_{opt}(r) = V_{st}(r) + V_{pol}(r) + iV_{abs}(r), \tag{6}$$

where $V_{st}(r)$ is the static potential, $V_{pol}(r)$ is the polarization potential and $V_{abs}(r)$ is the absorption potential. All these potentials are dependent on atomic charge density. The

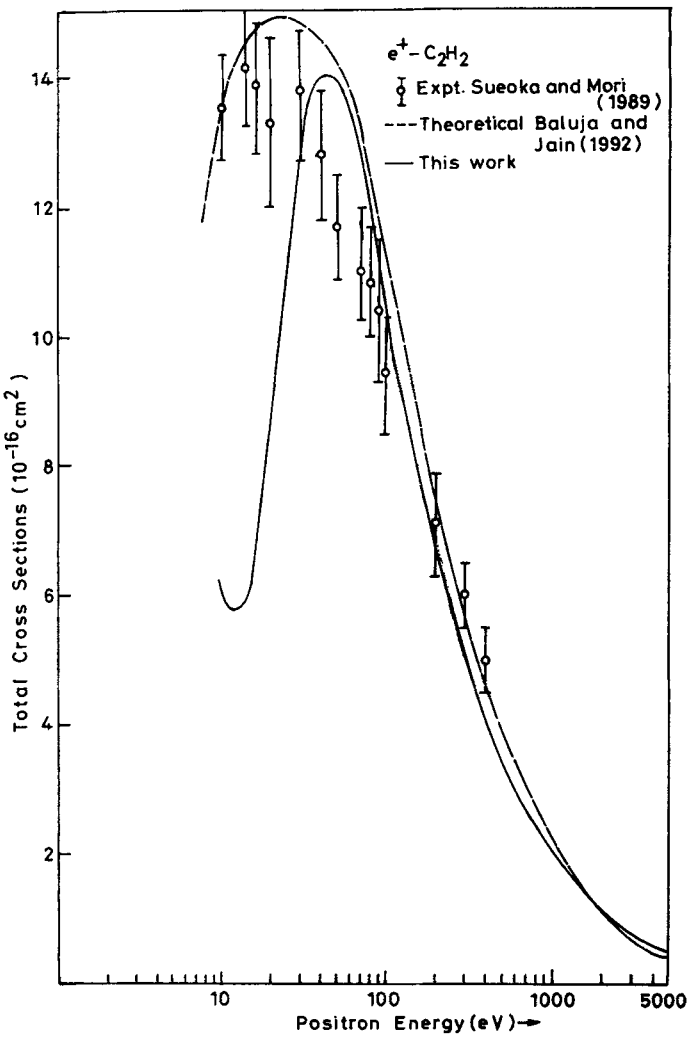

Figure 2. Total cross-sections for positron impact on C_2H_2.

static potential $V_{st}(r)$ is repulsive and is calculated at the Hartree–Fock level by employing the independent-particle model [19] and is parameterized as

$$V_{st}(r) = \frac{Z}{r}\Omega(r), \tag{7}$$

where

$$\Omega(r) = [h(e^{r/d} - 1) + 1]^{-1}. \tag{8}$$

It may be noted that this static potential for scattering from neutrals, decays exponentially. The parameter d and h for carbon are 0·88 and 1·759 respectively. For hydrogen,

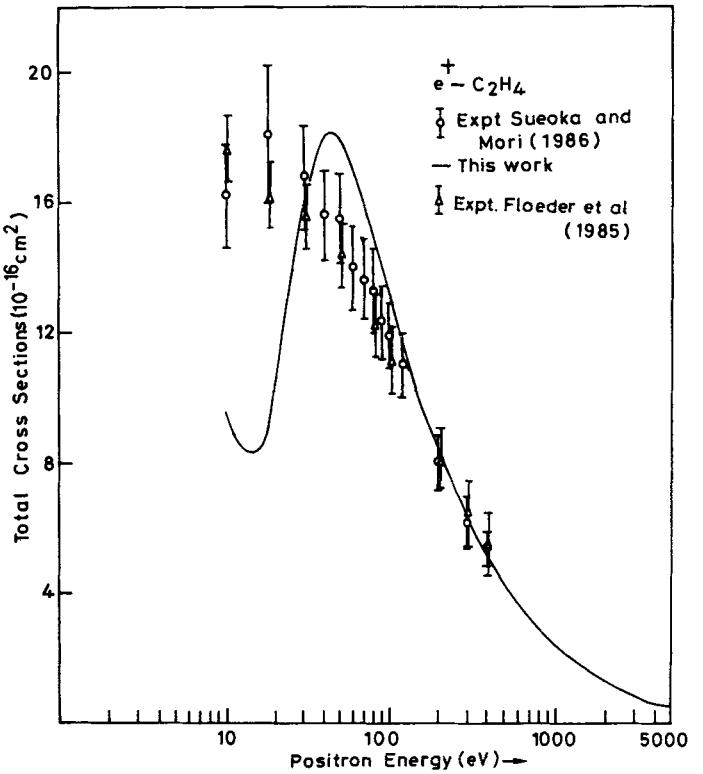

Figure 3. Total cross-sections for positron impact on C_2H_4.

$V_{st}(r)$ is calculated exactly and is given by [20]

$$V_{st}(r) = \left(1 + \frac{1}{r}\right) e^{-2r}. \tag{9}$$

The polarization potential $V_{pol}(r)$ is based on the correlation energy of a single positron in an inhomogeneous electron gas [21]. This polarization is different from the corresponding electron case [22], because the positron distorts the electronic charge cloud differently from the corresponding electron case. Near the nucleus, the two polarizations differ, whereas asymptotically they both behave as $-(\alpha/2r^4)$ where α is the static dipole polarizability of the atom. The correlation energy is calculated from the ground state expectation value of the hamiltonian which describes the fixed positron interacting with the target electrons. The positron polarization potential has been interpolated for the whole radial region and is dependent only on the target density via a density parameter r_s, where

$$\frac{4\pi}{3} r_s^3 \rho(r) = 1. \tag{10}$$

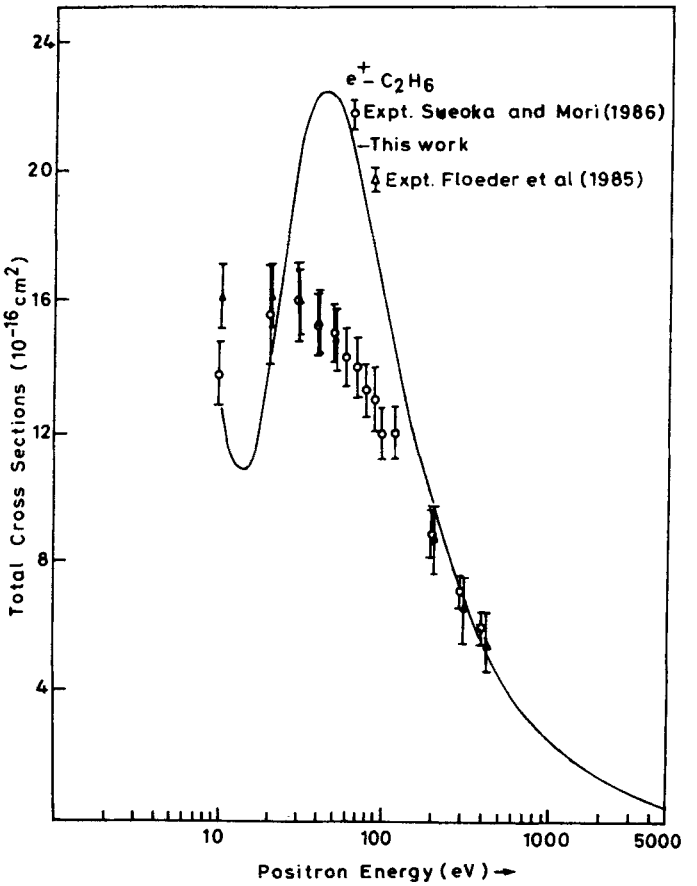

Figure 4. Total cross-sections for positron impact on C_2H_6.

The expressions for different radial regions have already been given [18]. The density $\rho(r)$ for carbon is taken from the independent-atom model [19]

$$\rho(r) = ((Z-1)/4\pi r^2 d)\xi[he^{\xi}/(1+hT)^2][-1+2he^{\xi}/(1+hT)], \tag{11}$$

where $T = e^{\xi} - 1$ and $\xi = r/d$. For carbon, $\alpha = 11{\cdot}878a_o^3$. The imaginary part $V_{abs}(r)$ represents the total loss of flux into all accessible channels. We have employed the semi-empirical form [23–26] of electron case V^-_{abs} modified for positron case $V^+_{abs}(r)$ as prescribed earlier [18]. They are related as

$$V^+_{abs}(r) = \frac{2}{\sqrt{kr}} V^-_{abs}(r). \tag{12}$$

This particular form has been shown to give good results for total cross sections for positron impact on several molecules. The factor 2 accounts for the fact that exchange is

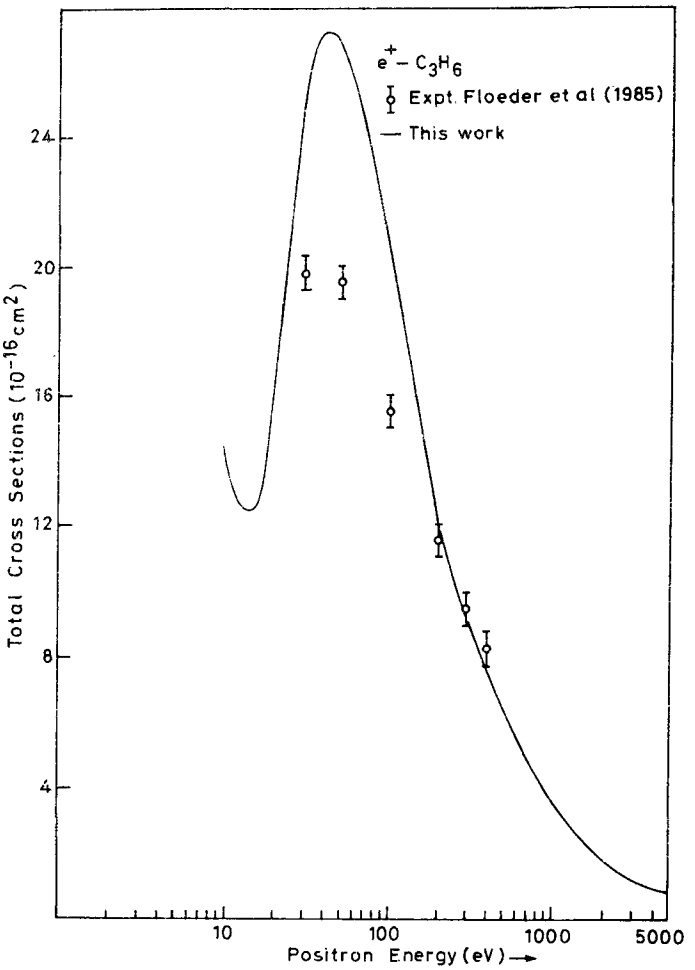

Figure 5. Total cross-sections for positron impact on C_3H_6.

absent in positron scattering. It may be pointed out that a factor of 1/2 approximately accounts for exchange effects in the evaluation of $V^-_{abs}(r)$. So to remove this factor, a factor of 2 appears in $V^+_{abs}(r)$. The factor $1/\sqrt{kr}$ approximately accounts for Ps formation at lower energies. It is now a standard procedure to solve the radial Schrödinger equation. We transform this equation into a set of first order coupled differential equations for the real and imaginary parts of the complex phase functions. These equations are solved by a variable phase approach. The S matrix and the elastic and inelastic cross sections are evaluated by standard formulas [18]. The positron-atom scattering total cross sections are obtained by summing the elastic and inelastic components.

The number of partial waves included depend upon the energy of the incident positron. At 5000 eV, 400 partial waves are used. After 30 partial waves, the polarized

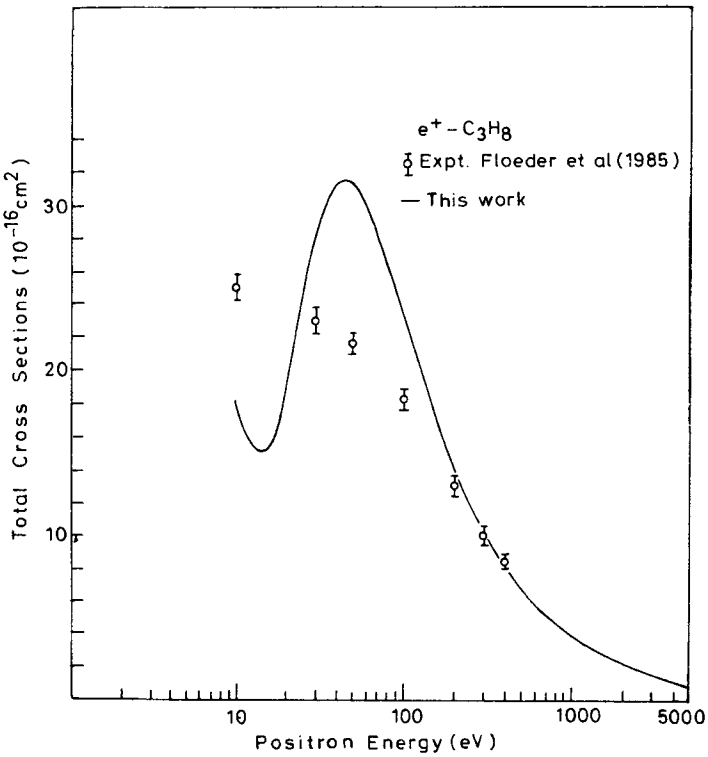

Figure 6. Total cross-sections for positron impact on C_3H_8.

Born phase shifts are employed. The integration is carried up to a radius where all the components of the interacting potentials are negligible. Convergence was tested by taking various step sizes.

3. Results and discussion

In figure 1, we display the theoretical e^+–CH_4 total cross section values (σ_t) in the energy range 10–5000 eV along with the experimental points of Floeder *et al* and Seuoka and Mori [15]. Floeder *et al* [14] measured σ_t values in a transmission experiment utilizing positrons from a ^{22}Na source and a tungsten moderator. They obtained σ_t values in the energy range 5–400 eV for various hydrocarbons like methane, ethane, ethene, propane, propene, cyclopropane, *n*-butane, isobutane and l-butene. Seuoka and Mori [15] measured σ_t values for methane, ethane and ethylene in the energy range 0·7–400 eV by using a retarded potential time of flight method. Their values were not absolute but were normalized to e^+–N_2 data [27]. We notice that our peak in σ_t occurs at 50 eV against experimental peak at 30 eV. Beyond 100 eV, we are in good accord with both the experiments, The effect of rotational excitation is expected to be small for this spherical hydride because the first non vanishing moment is

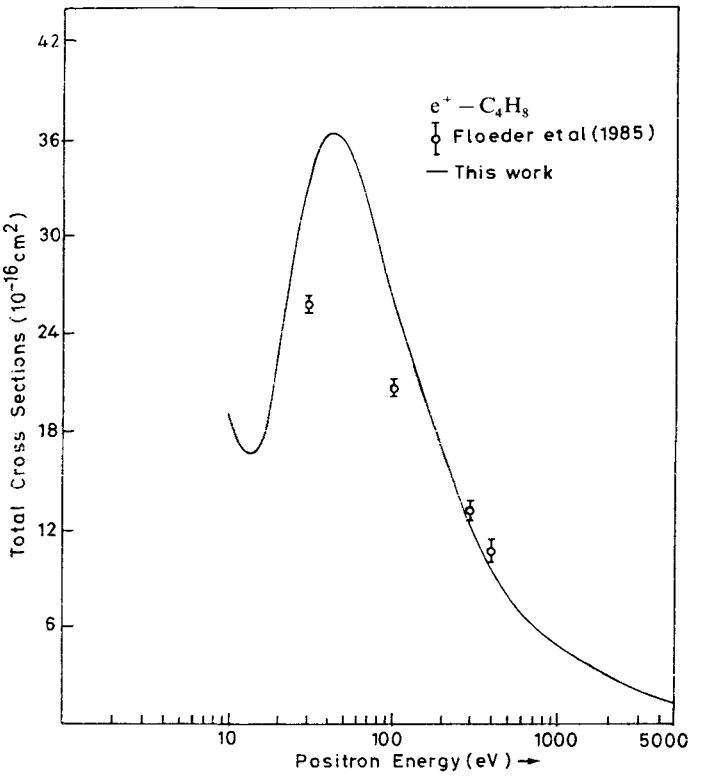

Figure 7. Total cross-sections for positron impact on C_4H_8.

octupole in nature. We also compare our theoretical values with that obtained by Baluja and Jain [1] in which the optical potential was determined from the molecular wave function at the Hartree–Fock level. The good agreement between the two theoretical curves indicate that the role of bonding is not significant at higher energies for this spherical system. There are other experimental data available [28, 29] for e^+–CH_4 cross sections but we have not shown these because these experimental points almost coincide with the experimental data shown in figure 1.

In figure 2, we display σ_t values for e^+–C_2H_2 scattering system along with the experimental points [17]. The values reproduce the hump at 40 eV. Excellent agreement was obtained with the experiment beyond 80 eV. The values in the low energy region are not in good agreement with the experimental results. This shows that the rule of additivity is not reliable at low energies. Since C_2H_2 is a linear molecule, the rotational excitation may not be insignificant in the low energy region. We obtained good agreement with other calculation [1] which employed molecular wavefunctions. This once again reveals that the effect of bonding is not very significant. In figures 3 and 4, we have shown σ_t values for e^+–C_2H_4 and e^+–C_2H_6 system respectively along with the experimental points [15]. For C_2H_4, we have excellent agreement with the experiment beyond 80 eV. However, for C_2H_6 we are in good accord with the

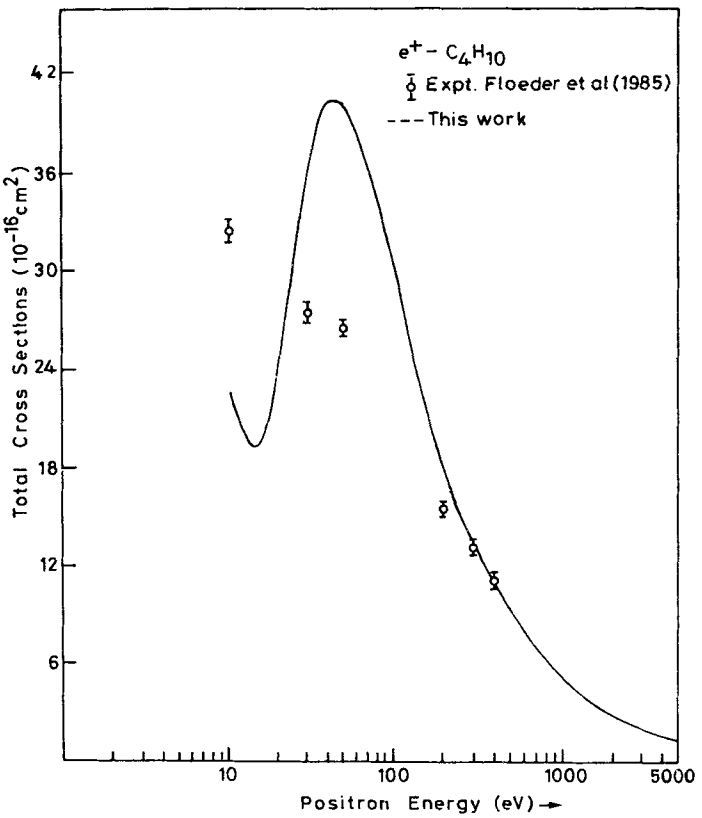

Figure 8. Total cross-sections for positron impact on C_4H_{10}.

experiment only beyond 100 eV. For C_2H_6 our points are higher than the experimental points in the energy range 30–100 eV. Our additivity rule predicts $\sigma_t(C_2H_6) > \sigma_t(C_2H_4)$, but the experimental points reveal the trend $\sigma_t(C_2H_6) < \sigma_t(C_2H_4)$ for positron impact energies below 50 eV. This is perhaps due to the fact that the electronic orbits in ethane molecules are saturated in comparison to ethylene. A similar situation prevails for C_3H_6, C_3H_8, C_4H_8, C_4H_{10} and C_6H_6.

These results are shown in figures 5–9 respectively along with experimental results [14, 16]. For all these cases, we have good agreement with the experimental results beyond 100 eV. Our extensive study on these hydrocarbons indicate that the rule of additivity is able to predict good cross sections for energies beyond 100 eV. Our model predicts the same cross sections for different isomers of a hydrocarbon. For example, the total cross sections for *n*-butane and isobutane are identical. In fact this is borne out by the experimental results [14] which further lends support to our additivity model.

We have calculated the total cross sections for positron impact on hydrocarbons by the following form

$$\sigma_t(C_nH_m) = naE^{-b} + mcE^{-d} \tag{13}$$

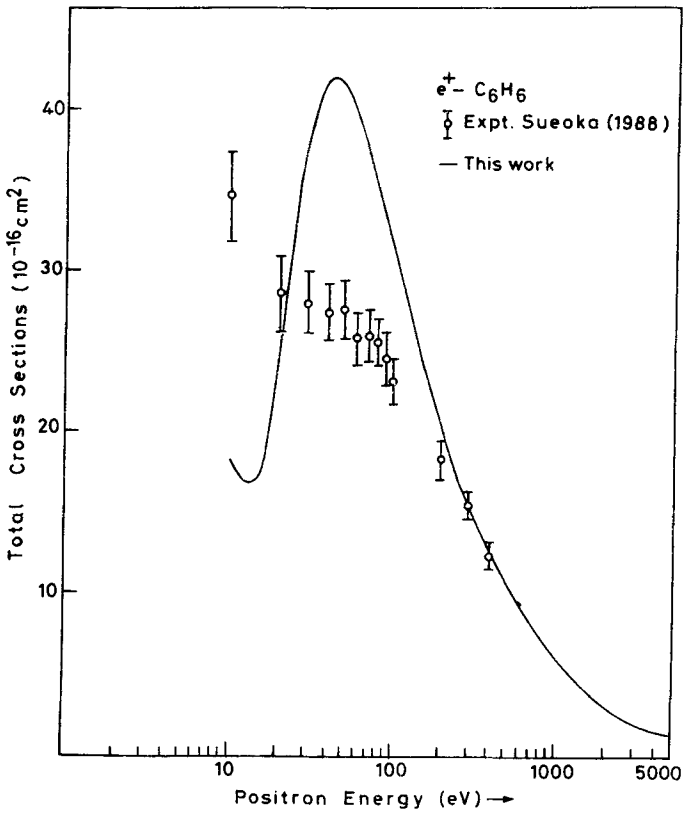

Figure 9. Total cross-sections for positron impact on C_6H_6.

where a and b refer to the fit of total cross sections for carbon atom; and c and d refer to the hydrogen atom. The values of these constants are $a = 195{\cdot}0543$, $b = 0{\cdot}7986$, $c = 371{\cdot}1757$ and $d = 1{\cdot}1379$. E is in eV and σ_t is 10^{-16} cm^2. The fit is valid in the energy range 300–5000 eV and is better than 5% in the energy range 300–5000 eV.

In figure 10, we have displayed our absorption cross sections, σ_{abs}, for e^+ impact on H_2. We have compared our results with the calculations of optical model potential [1] in which molecular wavefunctions for H_2 were used to generate the potentials. The experimental results [30] are also shown. The measured points are a sum of the ionization cross sections and the Ps formation. The information on other inelastic channels like excitation and dissociation is lacking, so it is not taken into account. Our low energy (below 50 eV) results are lower than the molecular wavefunction results due to the use of different thresholds used. The calculations involving molecular wavefunctions used 8·62 as the Ps threshold whereas we used ionization potentials for hydrogen atom as the threshold value. The peaks in σ_{abs} differ by about 10 eV for the two calculations. At energies beyond 50 eV, the two curves seem to merge. Moreover, our theoretical curve is in better agreement with the experimental results. This implies that

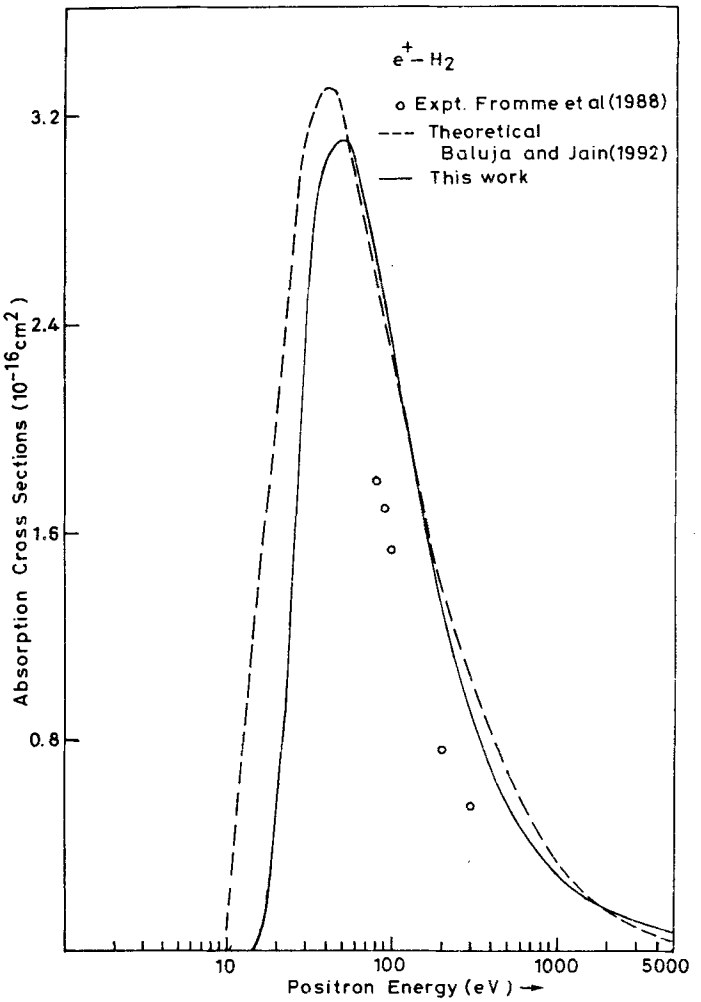

Figure 10. Absorption cross-sections for positron impact on H_2.

the ionization channel is the dominant one among all inelastic channels since Ps formation cross sections is very small at energies above 80 eV. Both the theoretical curves give an upper bound to the ionization cross sections because the ionization-cross sections is one of the components of the absorption cross section.

Our σ_{abs} cross sections for C_2H_2 are shown in figure 11 along with the molecular wavefunction calculations [1] employing a model optical potential approach using 4·61 eV as the threshold value. We used ionization potentials for H (13·605 eV) and C (11·26 eV) as thresholds for the addivity rule. As seen from figure our result lies lower than the molecular wave function calculation due to our high threshold value. At energies above 100 eV the two curves are very close to each other. Our simple model exhibits a peak at 50 eV which is 20 eV higher than the peak given by the other

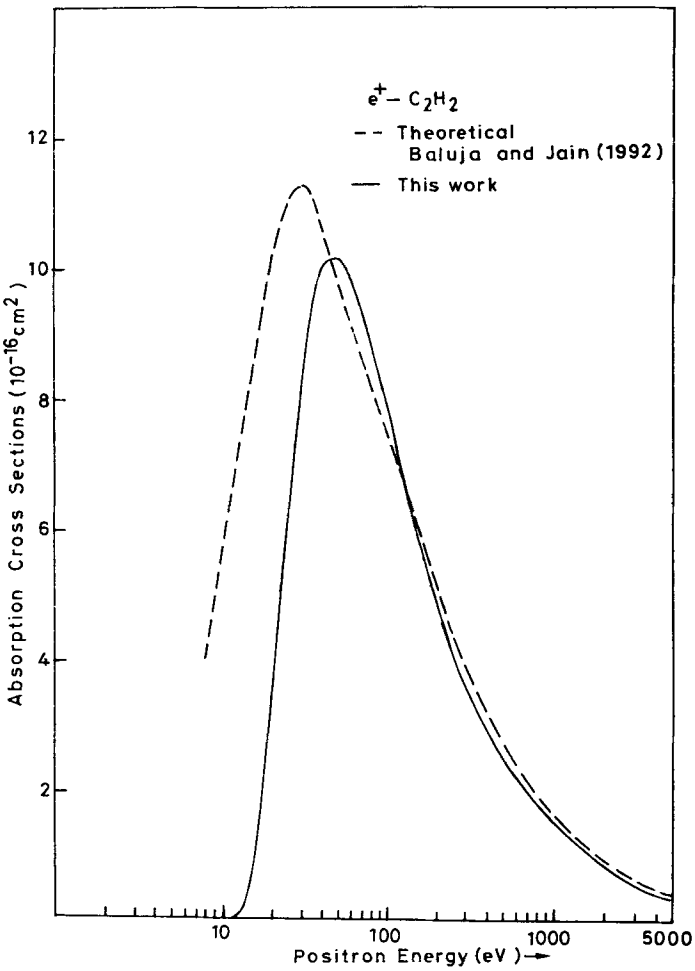

Figure 11. Absorption cross-sections for positron impact on C_2H_2.

calculation. There are no experimental results available for inelastic cross sections for C_2H_2.

The σ_{abs} cross sections for the methane molecule are shown in figure 12 along with the other calculation employing molecular wavefunctions [1], which used 6·18 eV as the threshold value. Once again due to the difference in threshold values used in the two theoretical models, our peak lies higher by about 20 eV. Beyond 100 eV, the two curves are in good accord with each other. There is no experimental information available for inelastic channels for this molecule. However, since the ground state of CH_4 is a singlet state and all the excited singlet states are repulsive in nature, we expect absorption cross sections to be very near to the ionization cross sections plus the dissociation cross sections for these excited states. These cross sections are not available for positron impact on CH_4. However, we have displayed the corresponding electron cross sections.

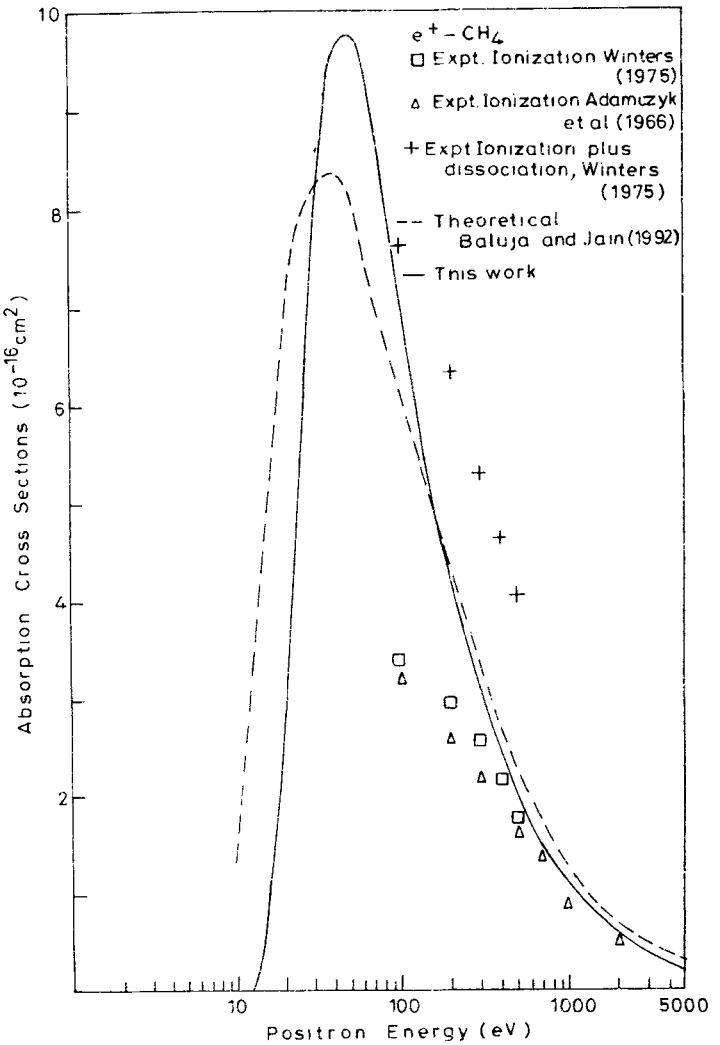

Figure 12. Absorption cross-sections for positron impact on CH_4.

The measured ionization cross sections [31,32] and the ionization plus dissociation cross sections [32] are shown. The absorption cross sections lie between ionization cross sections and the ionization plus dissociation cross sections. It is interesting to note that the absorption cross sections merge with the electron ionization cross section results at energies above 400 eV. It is well-known that at high energies, the ionization cross sections for electron and positron impact are nearly equal. This is due to the fact that according to first order perturbation theory, the Born cross sections are independent of the charge of projectile. Due to the cancellation effect of the repulsive static potential for e^+–CH_4 and the attractive polarization potential, the positron cross sections are lower than electron case. So we expect that the total ionization cross

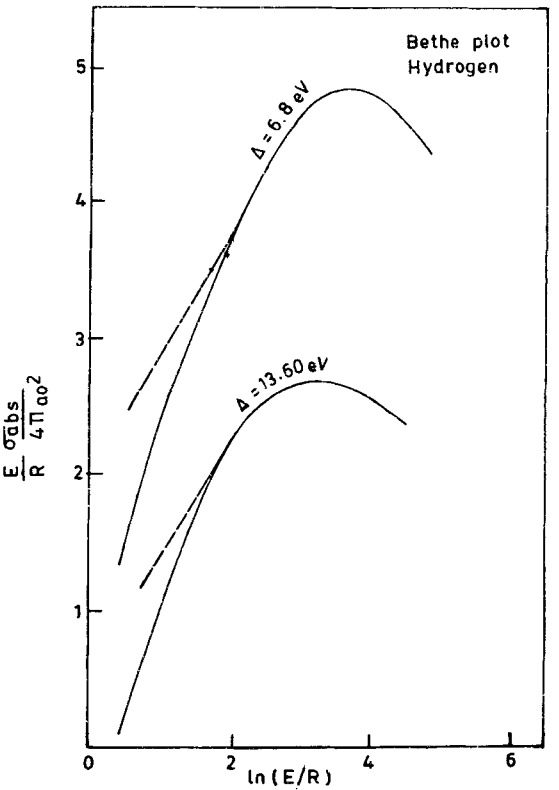

Figure 13. Bethe plot for positron impact on H.

sections plus the dissociation cross sections for the positron case would be lower than the electron case and the expected results may lie on our absorption curve.

It is well-known from Bethe's asymptotic theory of inelastic scattering that the total inelastic cross sections can be parametrized in the form

$$\sigma_{abs} = \frac{4\pi a_0^2}{(E/R)}\left[M_{tot}^2 \ln\left(4C_{tot}\frac{E}{R}\right)\right], \tag{14}$$

where R is the Rydberg energy. The constant M_{tot}^2 is the total dipole matrix element squared and is related to $S(-1,0)$ [33]. The equation suggests that a plot between $\sigma_{abs}(E/R)/4\pi a_0^2$ against $\ln(E/R)$ is a straight line which is known as Bethe plot. We have shown these plots for positron impact on hydrogen and carbon in figures 13 and 14 respectively. The Bethe parameter for hydrogen are $M_{tot}^2 = 0{\cdot}846$, $C_{tot} = 0{\cdot}479$ and for carbon these are $M_{tot}^2 = 2{\cdot}59$ and $C_{tot} = 0{\cdot}309$. M_{tot}^2 is obtained by using the linear portion of the Bethe plots. It is worth mentioning that these parameters have been derived when the threshold is kept at the ionization limit, and we observe that the law of additivity gives good results for positron impact on hydrocarbons. When the threshold

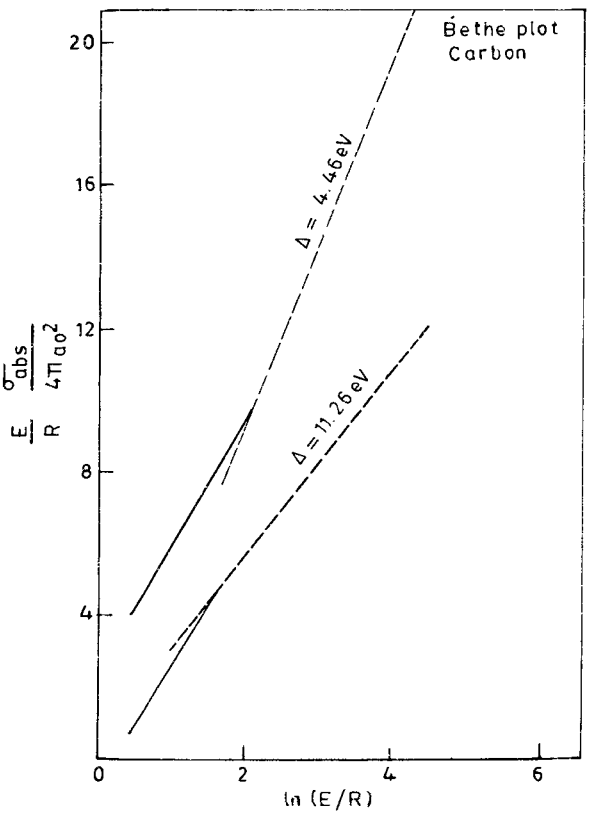

Figure 14. Bethe plot for positron impact on C.

is kept at the energy of positronium formation, then for hydrogen we get $M^2_{tot} = 0{\cdot}909$, $C_{tot} = 2{\cdot}2567$ and for carbon we get $M^2_{tot} = 5{\cdot}45$, $C_{tot} = 0{\cdot}1708$. Our value of M^2_{tot} for hydrogen agrees with the exact value of $M^2_{tot} = 1{\cdot}0$ [33], which can be calculated by evaluating $S(-1, k) = (k)^{-2}[1 + (1 + k^2/4)^{-4}]$ in the limit $k \to 0$. In the closure approximation $M^2_{tot} = Z/\Delta(\text{Ryd})$, where Δ is the mean excitation energy of the atom with Z electrons, Δ can be calculated with the knowledge of the polarizability α_d and the value of $\langle r^2 \rangle$ by the relation $\alpha_d = (2/3)(\langle r^2 \rangle/\Delta)$. For carbon atom, $\alpha_d = 11{\cdot}878 a_0^3$, and $\langle r^2 \rangle = 13{\cdot}7372 a_0^2$ at the Hartree–Fock level and we get $\Delta = 20{\cdot}98\,\text{eV}$. This yields $M^2_{tot} = 3{\cdot}89$. The total dipole element squared M^2_{tot} can also be known from the knowledge of oscillator strengths and the relevant energy levels and the value of M^2_{ion}. For carbon atom, we consider only the first three excited states $1s^2 2s2p\,^3D^0 P^0$ and $^3S^0$ which have their energy levels at $64089\,\text{cm}^{-1}$, $75255\,\text{cm}^{-1}$ and $105799\,\text{cm}^{-1}$ with respect to the ground state $1s^2 2s^2 2p^2\,^3P^e$.

The values of oscillator strengths for these transitions from the ground state are respectively 0·1, 0·1, 0·25. The total contribution of these three states is 0·5764 to the value of M^2_{tot}. To get the contribution M^2_{ion} of ionization; we made Bethe plot using the

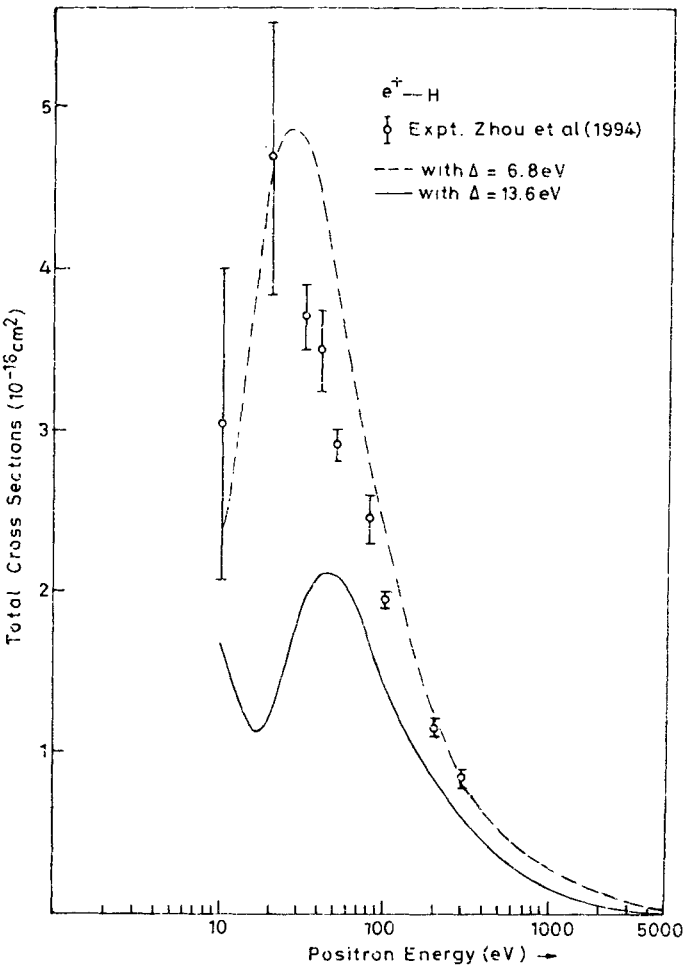

Figure 15. Total cross-sections for positron impact on H.

ionization cross sections values [34]. We obtained $M^2_{ion} = 3{\cdot}96$ giving $M^2_{tot} = 4{\cdot}54$. This value is derived from electron data and is of comparable magnitude with our positron value of $M^2_{tot} = 5{\cdot}45$. We emphasize that our optical model potential is capable of giving good values of the absorption cross sections and the total cross sections for hydrogen and carbon atoms provided the threshold is kept at the Ps formation threshold. However, the rule of additivity works for hydrocarbons only if the threshold is kept at the ionization limit. We also display our total cross section results for hydrogen and carbon in figures 15 and 16 respectively. We compare our results for hydrogen with the experimental results [35] and we notice good agreement beyond 80 eV.

In conclusion, we state that the rule of additivity works well for positron impact on hydrocarbons when the total cross sections for the constituent atoms are calculated by

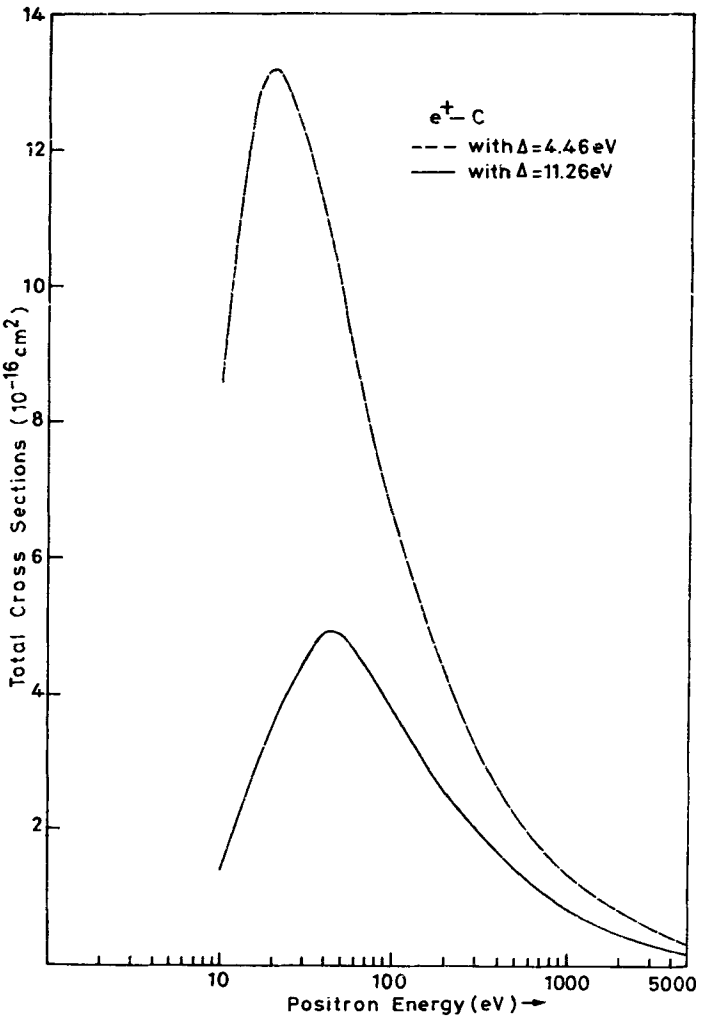

Figure 16. Total cross-sections for positron impact on C.

employing an optical model potential and the absorption potential is calculated by keeping the threshold at the ionization limit.

References

[1] K L Baluja and A Jain, *Phys. Rev.* **A45**, 7838 (1992)
[2] T S Stein and W E Kauppila, in *Electronic and atomic collisions*, edited by D C Lorentz *et al* (Elsevier, New York, 1986) p. 105
[3] C Szmytkowski, *Z. Phys.* **D13**, 69 (1989)
[4] O Sueoka, in *Atomic physics with positrons*, edited by J W Humberston and E A G Armour (Plenum, New York, 1987), p. 41

[5] E A G Armour, *Phys. Rep.* **169**, 1 (1988)
[6] H S W Massey, E H S Burhop and H B Gilbody, *Electronic and ionic impact phenomena* (Clarendon, Oxford, 1969) Vol II
[7] C J Joachain, *Quantum collision theory* (North Holland, Amsterdam, 1979) Vol. 1
[8] K N Joshipura and P M Patel, *Pramana – J. Phys.* **39**, 293 (1992)
[9] K N Joshipura and P M Patel, *Z. Phys.* **D29**, 269 (1994)
[10] S K Tyagi, Total cross-sections for electron scattering by hydrocarbons, M Phil. Thesis, Meerut University (1993)
[11] O J Orient and S K Srivastava, *J. Phys.* **B20**, 3923 (1987)
[12] S M Younger and T D Mark, *Electron impact ionization* (Springer, Berlin, 1985) Vol I
[13] B H Bransden, *Atomic collision theory* (Benjamin/Cummings Reading, M A, 1983)
[14] K Floeder, D Fromme, W Raith, A Schwab and G Sinapius, *J. Phys.* **B18**, 3347 (1985)
[15] O Sueoka and S Mori, *J. Phys.* **B19**, 4035 (1986)
[16] O Sueoka, *J. Phys.* **B21**, L361 (1988)
[17] O Sueoka and S Mori, *J. Phys.* **B22**, 963 (1989)
[18] K L Baluja and A Jain, *Phys. Rev.* **A46**, 1279 (1992)
[19] A E S Green, D L Sellin and A S Zachor, *Phys. Rev.* **184**, 1 (1969)
[20] P G Burke, *Potential scattering in atomic physics* (Plenum Press, New York, 1977)
[21] A Jain, *Phys. Rev.* **A41**, 2437 (1990)
[22] J K O'Connell and N F Lane, *Phys. Rev.* **A27**, 1893 (1983)
[23] G Staszewska, D W Schwenke, D Thirumalai and D G Truhlar, *J. Phys.* **B16**, L281 (1983)
[24] G Staszewska, D W Schwenke, D Thirumalai and D G Truhlar, *Phys. Rev.* **A28**, 2740 (1983)
[25] G Staszewska, D W Schwenke and D G Truhlar, *J. Chem. Phys.* **81**, 335 (1984)
[26] G Staszewska, D W Schwenke and D G Truhlar, *Phys. Rev.* **A29**, 3078 (1984)
[27] K R Hoffman, M S Dababneh, Y F Hsieh, W E Kauppila, V Pol, J H Smart and T S Stein, *Phys. Rev.* **A25**, 1393 (1982)
[28] M Charlton, T C Griffith, G R Heyland and G L Wright, *J. Phys.* **B13**, L353 (1980)
[29] M S Dababneh, Y F Hsieh, W E Kauppila, C K Kwan, S J Smith, T S Stein and M N Uddin, *Phys. Rev.* **A38**, 1207 (1988)
[30] D Fromme, G Kruse, W Raith and G Sinapius, *J. Phys.* **B21**, L261 (1988)
[31] B Adamczyk, A J H Boerboom, B L Schram and J Kistemaker, *J. Chem. Phys.* **44**, 4640 (1966)
[32] H F Winters, *J. Chem. Phys.* **63**, 3462 (1975)
[33] M Inokuti, *Rev. Mod. Phys.* **43**, 297 (1971)
[34] K Omidvar, H L Kyle and E C Sullivan, *Phys. Rev.* **A5**, 1174 (1972)
[35] S Zhou, W E Kauppila, C K Kwan and T S Stein, *Phys. Rev. Lett.* **72**, 1443 (1994)